Kinetics of Fluid Demixing in Complex Plasmas: Role of Two-Scale Interactions

A. Wysocki,[1] C. Räth,[2] A. V. Ivlev,[2,*] K. R. Sütterlin,[2] H. M. Thomas,[2] S. Khrapak,[2] S. Zhdanov,[2] V. E. Fortov,[3] A. M. Lipaev,[3] V. I. Molotkov,[3] O. F. Petrov,[3] H. Löwen,[1] and G. E. Morfill[2]

[1]*Heinrich-Heine-Universität Düsseldorf, 40225 Düsseldorf, Germany*
[2]*Max-Planck-Institut für Extraterrestrische Physik, 85741 Garching, Germany*
[3]*Joint Institute for High Temperatures, 125412 Moscow, Russia*

(Received 27 March 2010; published 21 July 2010)

Using experiments and combining theory and computer simulations, we show that binary complex plasmas are particularly good model systems to study the kinetics of fluid-fluid demixing at the ''atomistic'' (individual particle) level. The essential parameters of interparticle interactions in complex plasmas, such as the interaction range(s) and degree of nonadditivity, can be varied significantly, which allows systematic investigations of different demixing regimes. The critical role of competition between long-range and short-range interactions at the initial stage of the spinodal decomposition is discussed.

DOI: 10.1103/PhysRevLett.105.045001 PACS numbers: 52.27.Lw

When a binary fluid is quenched into the immiscible state, it starts to dynamically demix until the thermodynamically stable state of two coexisting fluids is reached. The spinodal decomposition is accompanied by a sequence of domain growth regimes which are believed to be self-similar in time; i.e., the domain morphology (within each regime) is preserved [1–4]. This implies a single time-dependent characteristic length which obeys a power-law growth $L(t) \propto t^{\alpha}$, with distinct growth exponents α peculiar to each regime.

Competing interactions play a very important role in the morphology of separating phases, resulting in a rich variety of domain patterns ranging from striped lamellar structures to hexagonal arrays of droplets [5] and clusters [6]. The asymptotic evolution (characterized by sharp interfaces between domains) in systems with such interactions is governed by the competition between the long-range repulsion stimulating subdivision of domains and the short-range (effective) attraction resulting in the growth of interfacial energy. There has been a great deal of theoretical research of this process carried out in the mean-field framework (by using the modified Ginzburg-Landau formalism, e.g., [7,8]). However, there are very few particle-resolved studies of such systems [9], in particular, addressing the role of competing interactions.

Complex plasmas are composed of a weakly ionized gas and microparticles which are highly (negatively) charged due to absorption of the ambient electrons and ions [10,11]. Binary complex plasmas contain microparticles of two different sizes (charge is approximately proportional to size) and constitute a model system which is very well suited for studying the kinetics of fluid demixing at the individual particle level: Properties of pair interactions in such systems can be flexibly tuned, and the interaction range can be made very long (much longer than the mean interparticle distance) [10,12]. Moreover, the dynamics of individual particles at short time scales is virtually undamped, because the background gas in complex plasmas is typically very dilute [11]. These properties of complex plasmas provide perfect complementarity to the colloid-polymer mixtures [13] where the interparticle interactions are usually of a short range and the individual particle dynamics is damped by the host fluid.

In this Letter, we report on the first-ever series of dedicated experiments which demonstrate the very strong tendency for binary complex plasmas to demix. Such experiments provide us with a unique opportunity to observe both species of demixing binary system at the individual particle level. Furthermore, using particle-resolved Langevin simulations we show that for binary fluids with competing short-range and long-range repulsive interactions (also typical to complex plasmas) the onset of the spinodal decomposition is different from that in fluids with short-range interactions. Instead of the regular growth sequence [14]—the initial diffusive regime with $\alpha = 1/3$ crossing over into the hydrodynamic viscous regime with $\alpha = 1$—the long-range interactions can shortcut the initial evolution: The diffusive growth is replaced with the emergence of domains of (almost) time-independent length ''preset'' by the interaction range. During this ''plateau'' regime L is much larger than the short-range correlation length (which usually characterizes the initial scale at the diffusive growth), and interfaces between the domains sharpen until the surface tension drives the transition in a coarsening viscous growth.

To study the principal possibility of phase separation in binary complex plasmas, we performed experiments with the PK-3 Plus rf discharge chamber [15] on board the International Space Station. In the experiments carried out at different discharge conditions (discharge power and gas pressure), we used various combinations of ''big'' and ''small'' monodisperse particles (in the range from 1.55 to 9.2 μm). After the injection, small particles were driven through a stationary cloud of big ones (by a weak electric field existing in the discharge). When the small particles approached the center of the chamber and thus the driving

field practically vanished, an apparent phase separation was observed (within 1–2 seconds) accompanied by the formation of a small-particle droplet with a well-defined spheroidal shape, as illustrated in Fig. 1 (see also supplemental movie S1 [16]). These experiments demonstrate that binary complex plasmas have a very strong tendency to demix at time scales of seconds. Below, we identify the generic (thermodynamic) mechanisms which are responsible for this process.

The prevailing mechanism of interaction between charged microparticles in complex plasmas is electric repulsion [10,11]. The particle screening is provided by the ambient electrons and ions and occurs in an extended region which can be a few orders of magnitude larger than the particle itself. Moreover, the size of microparticles is typically very small in comparison with the interparticle distance. Therefore, we can treat particles as pointlike. At large distances r, the electrostatic potential of a particle can be represented in the asymptotic form $\phi(r) = Z^*(Z)Y(r)$, expressed via the effective charge Z^* [which is determined by the dominating screening mechanism(s) and thus is a certain function of the actual charge Z] and the dominating asymptotic profile $Y(r)$ (independent of Z) [17]. For a binary system, with particles "1" and "2" characterized by the actual charges Z_1 and Z_2, respectively, this yields the (asymptotic) pair interaction energy $V_{ij}(r) = \frac{1}{2}(Z_i Z_j^* + Z_j Z_i^*)Y(r)$, $i, j = 1, 2$. From the generalized Berthelot mixing rule $V_{12} = (1 + \delta)\sqrt{V_{11}V_{22}}$, one can readily derive the nonadditivity parameter δ and show that for arbitrary nonlinear dependence $Z^*(Z)$ it is always positive. Thus, demixing of binary complex plasmas is always stimulated [17].

Theory predicts a rich variety of screening mechanisms operating in complex plasmas [10,12]. The shape of $\phi(r)$ can be affected by the plasma absorption on a particle, nonlinearity in plasma-particle interactions, ionization-loss balance, etc. Recently, it was shown that the plasma production and loss processes can play a crucial role in the long-range behavior of $\phi(r)$ [18]. This results in the emergence of two dominating asymptotes of $\phi(r)$—both having the Yukawa form, so that we will refer to it as a double-Yukawa repulsive potential:

$$\phi(r) = \frac{1}{r}(Z_{\mathrm{SR}}^* e^{-r/\lambda_{\mathrm{SR}}} + Z_{\mathrm{LR}}^* e^{-r/\lambda_{\mathrm{LR}}}). \quad (1)$$

It is remarkable that the length scales λ_{SR} and λ_{LR} can be very different, and therefore we denoted them as "short-range" (SR) and "long-range" (LR). Typically, λ_{SR} is determined by the classical mechanism of Debye-Hückel screening, and the dependence of Z_{SR}^* on Z is governed by the screening nonlinearity [17]. Therefore, λ_{SR} is of the order of the plasma Debye screening length, which is normally smaller than the mean interparticle distance Δ. In contrast, the magnitude of λ_{LR} as well as the dependence $Z_{\mathrm{LR}}^*(Z)$ is controlled by the balance between the plasma production and loss. Therefore, λ_{LR} can vary over a fairly broad range and is usually much larger than Δ. Furthermore, the ratio $Z_{\mathrm{LR}}^*/Z_{\mathrm{SR}}^* \equiv \epsilon$ is typically small (both effective charges are negative) [18]. For a binary system, Eq. (1) yields the pair interaction energy ($i, j = 1, 2$; $\beta = \mathrm{SR}, \mathrm{LR}$): $V_{ij}(r) = \frac{1}{2r}\sum_\beta (Z_i Z_{\beta,j}^* + Z_j Z_{\beta,i}^*)e^{-r/\lambda_\beta}$. Note that the (effective) nonadditivity parameter δ now depends on r (see the inset in Fig. 2).

Let us first evaluate the unstable region where binary fluids interacting via the potential (1) start demixing. For this purpose we shall employ the stability analysis of the

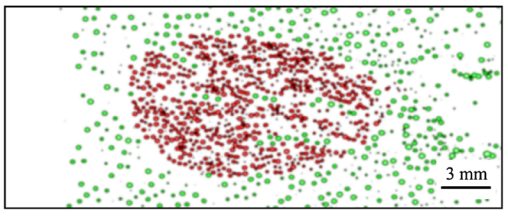

FIG. 1 (color online). Phase separation in binary complex plasmas. The figure illustrates one of the experiments performed under microgravity conditions in the PK-3 Plus rf discharge chamber (in argon discharge at a pressure of 30 Pa), with particles of 9.2 and 3.4 μm diameter. Small particles (red dots) were injected into a stationary cloud of big particles (green dots) and formed a spheroidal droplet which moved slowly towards the center of the chamber (to the right). The figure shows the longitudinal cross section; particles were illuminated by a thin laser sheet of $\simeq 0.35$ mm thickness.

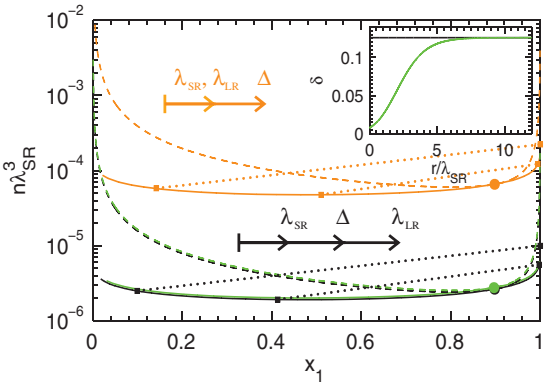

FIG. 2 (color). Phase diagram for binary fluids with the double-Yukawa repulsion (1). The phase variables are the reduced total particle density $n\lambda_{\mathrm{SR}}^3$ and the relative composition x_1 of species 1. Solid lines are the binodals, dashed lines are spinodals (critical points are marked by bullets), and dotted tie lines connect coexisting fluid states (marked by squares)—all obtained from the RPA approach. The calculations are for $\Gamma_1 = 6.4 \times 10^3$, $\epsilon = 0.2$ (for both species), and $\tilde{Z} = 2.7$. Three cases are illustrated, corresponding to different values of Λ and $\tilde{\nu}_{\mathrm{SR}}$: Orange lines are for $\Lambda = 1$, black are for $\Lambda = 12$; in both cases $\tilde{\nu}_{\mathrm{LR}} = \tilde{\nu}_{\mathrm{SR}} = 2.7$ (both LR and SR interactions are nonadditive); green lines show the case $\Lambda = 12$, but with $\tilde{\nu}_{\mathrm{LR}} = 2.7$ and $\tilde{\nu}_{\mathrm{SR}} = 1$ (only LR interactions are nonadditive). For the orange and black lines, the relations between λ_{SR}, λ_{LR}, and Δ (corresponding to Fig. 3, with the same color coding) are drawn schematically. The inset represents the effective nonadditivity parameter δ vs distance between particles (for black and green lines).

Ornstein-Zernike equation combined with the simplest random-phase approximation (RPA) closure relation [17,19]. This yields the spinodal

$$6\Gamma_1 n\lambda_{\mathrm{SR}}^3[\tilde{\nu}_{\mathrm{SR}} - 1 + \epsilon\Lambda^2(\tilde{\nu}_{\mathrm{LR}} - 1)]^2 x_1(1 - x_1) = \tilde{Z}^{-2}(1 + \epsilon\Lambda^2)x_1 + (\tilde{\nu}_{\mathrm{SR}} + \epsilon\Lambda^2\tilde{\nu}_{\mathrm{LR}})(1 - x_1). \quad (2)$$

Here $\Gamma_1 = Z_1^2\nu_{\mathrm{SR}}/(k_B T\lambda_{\mathrm{SR}})$ is the coupling parameter which characterizes the strength of the interaction between species 1 (k_B is the Boltzmann constant and T is the temperature), x_1 is the relative composition of species 1, and $n \equiv \Delta^{-3}$ is the total number density of particles. We also introduced the charge ratio $\tilde{Z} = Z_2/Z_1$ (for certainty we assume $\tilde{Z} > 1$) and the screening length ratio $\Lambda = \lambda_{\mathrm{LR}}/\lambda_{\mathrm{SR}}$. Finally, $\nu_{\mathrm{SR,LR}} = Z^*_{\mathrm{SR,LR}}/Z$ are the renormalizing charge ratios [17]: Their deviations from unity characterize the degree of nonadditivity for the SR and LR interactions; $\tilde{\nu}_{\mathrm{SR,LR}}$ denotes the ratio of $\nu_{\mathrm{SR,LR}}$ for the particles 2 to that for the particles 1.

Figure 2 illustrates the phase diagram obtained from the RPA for binary fluids with double-Yukawa interactions (1). Along with the spinodals, we plotted the corresponding coexistence lines (binodals). Let us analyze the relative contribution of the SR and LR interaction parts to the phase equilibrium. For this purpose we naturally chose an equal degree of nonadditivity for both parts, $\tilde{\nu}_{\mathrm{LR}} = \tilde{\nu}_{\mathrm{SR}}$, and varied the ratio of the screening lengths Λ. Equation (2) immediately shows that for $\epsilon\Lambda^2 \ll 1$ the SR interactions dominate and the spinodal $n_{\mathrm{sp}}(x_1)$ coincides with that derived for binary fluids with (single) Yukawa interactions [17]. The LR interactions dominate in the opposite limit $\epsilon\Lambda^2 \gg 1$, where $n_{\mathrm{sp}}(x_1)$ has the same (but rescaled) form. With the parameter set chosen for Fig. 2 the orange curves illustrate the "SR-dominated" case, and the black (and green) curves are for the "LR-dominated" case. This plot demonstrates that the LR interactions—although relatively weak—can significantly enhance demixing, which can also be deduced from Eq. (2): The spinodal for the LR-dominated case is obtained from the SR curve by dividing with the large factor $\sim\epsilon\Lambda^2$. One can also see that for $\epsilon\Lambda^2 \gg 1$ the SR nonadditivity has practically no effect on the equilibrium phase diagram (cf. black and green curves).

In order to investigate details of the atomistic dynamics accompanying the phase separation in binary complex plasmas and make the comparison with theory, we employed molecular dynamics (MD) simulations with the Langevin thermostat (see [16] for details). A binary mixture was composed of 729 000 particles (1 + 2) at the off-critical composition $x_1 = 0.5$. The simulations were performed in a cubic box with the dimensions of 27 mm (corresponds to $\Delta = 0.3$ mm) and periodic boundary conditions. The particles interacted via the potential (1), and the simulation parameters (approximately corresponding to the experiment shown in Fig. 1) are listed in the caption of Fig. 3.

The onset and the first stages of the phase separation were characterized by the evolving domain size $L(t)$, which was deduced from the time-dependent average structure factor $S(k, t)$ [2,4,20]. This is illustrated in Fig. 3, where $S(k, t)$ (for four different screening length ratios) is plotted at two characteristic moments of time. The position of maximum of $S(k)$ is identified as $2\pi/L$. One can see that even at the early stage of demixing (see inset) there is a clear trend for systems with larger Λ to demix faster, and at the later stage the difference becomes drastic. The position of maximum at each simulation time step was determined from the standard procedure [20], by using the off-critical fitting function $S(k) \propto (kL/2\pi)^2/[2 + (kL/2\pi)^6]$.

Figure 4 summarizes the results of our analysis (see also supplemental movies S2 and S3 [16]). In the SR-dominated case $\Lambda = 1$ [when Eq. (1) is reduced to the regular Yukawa form], the growth of domains of the minority phase 1 is rather slow [Figs. 4(b) and 4(c)], and the evolution of $L(t)$ [orange dots in Fig. 4(a)] is characterized by relatively small growth exponents, $\alpha \leq 0.17$ [21]. The interaction nonadditivity in this case is apparently too weak, so that domains remain fuzzy (at the simulation time scales) and their shape is fairly irregular. The characteristic width of the domain interfaces remains a significant fraction of L, which can explain the mismatch of the growth exponent with $\alpha = 1/3$ expected in the diffusive regime (which presumes negligibly narrow interfaces) [22,23]. The increase of Λ (i.e., of the interaction range) sharpens the interfaces and makes the domains grow faster—already at $\Lambda = 2$, where the SR and LR interactions contribute almost equally to the phase equilibrium, the growth exponent reaches the value of $\alpha \simeq 0.26$ [red dots in Fig. 4(a)].

A further increase of Λ (dominating LR interactions) causes a dramatic increase of the surface tension (see [16]). This results in earlier crossover to the viscous growth

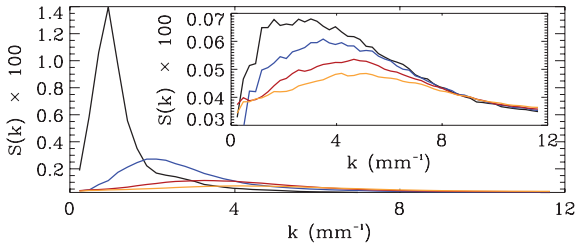

FIG. 3 (color). Average structure factor $S(k)$ upon the phase separation in fluids with the double-Yukawa repulsion (1). The results are from MD simulations for the off-critical composition $x_1 = 1/2$, with $Z_1 = 4000e$, $k_B T = 0.024$ eV, $\lambda_{\mathrm{SR}} = 150$ μm, and $\Delta = 0.3$ mm; the charge ratios are $\epsilon = 0.2$ and $\tilde{Z} = 2.7$ (as in Fig. 2). The curves are for four different ratios of the screening lengths: $\Lambda = 1$ (orange), 2 (red), 4 (blue), and 12 (black). For all cases, $\tilde{\nu}_{\mathrm{SR}} = \tilde{\nu}_{\mathrm{LR}} = 2.7$. The major plot is for the stage of developed phase separation, $t = 10$ s, while the inset shows $S(k)$ at the early stage of demixing, $t = 1$ s [marked in Fig. 4(a) by two vertical dashed lines].

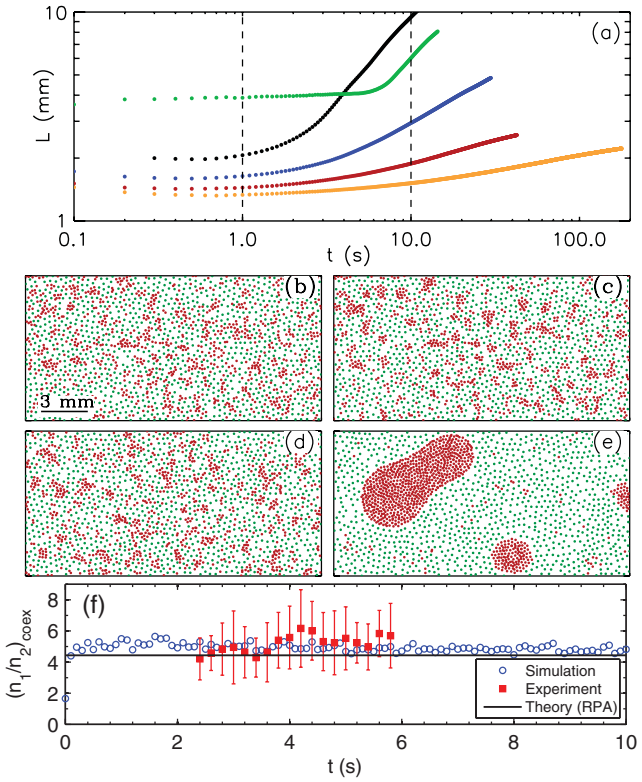

FIG. 4 (color). Kinetics of the phase separation in fluids with the double-Yukawa repulsion (1). The results are from MD simulations with the parameters of Fig. 3. The upper panel (a) shows the characteristic length of growing domains (of the minority phase 1) versus time $L(t)$, obtained for four different values of Λ (color coding of dots is the same as that of curves in Fig. 3). Green dots are for $\Lambda = 12$ with $\tilde{\nu}_{SR} = 1$ (only LR interactions are nonadditive). The middle panel shows the domain morphology for $\Lambda = 1$ (b),(c) and $\Lambda = 12$ (d),(e), particles 1 are color coded in red and particles 2 are green (slices of 0.3 mm are depicted). The left column represents the early stage of the phase separation, $t = 1$ s; the right column is for the developed stage, $t = 10$ s. The lower panel (f) shows the coexistence density ratio $(n_1/n_2)_{coex}(t)$ for $\Lambda = 12$.

regime [2,4], so that the diffusive regime can be completely preempted. Figures 4(d) and 4(e) illustrate this trend for $\Lambda = 12$: The initial small domains start to coarse rapidly at $t \gtrsim 2$ s (which is about the demixing time in the experiment), and $L(t)$ is almost linear at this stage ($0.9 \leq \alpha \leq 1.05$). As expected in this case, the coexistence density ratio $(n_1/n_2)_{coex}(t)$ tends to equilibrium [see Fig. 4(f)]: The ratios deduced from the experiment and simulation are practically constant and agree very well with the theoretical equilibrium value [16]. Note that the characteristic initial size $L(0)$ increases with Λ as well [see Fig. 4(a)].

It is noteworthy that the early stage of the phase separation kinetics is strongly affected by the nonadditivity of SR interactions—even in the LR-dominated regime. To illustrate this, we plotted $L(t)$ for simulations with $\Lambda = 12$ and additive SR interactions [green dots in Fig. 4(a)], whereas the LR interactions were kept nonadditive (the same as for black dots). One can see that "switching off" the SR nonadditivity results in a drastic increase of $L(0)$. Moreover, this "freezes out" the initial demixing kinetics—the domain size remains practically constant until $L(t)$ abruptly crosses over into the viscous growth regime, where the developments of the green and black curves are then almost the same. The relative importance of the SR and LR nonadditivity can be understood from Fig. 2: While the major plot demonstrates the practically coinciding phase boundaries for green and black curves, the inset suggests that when only LR interactions are nonadditive the effective nonadditivity starts operating at rather large r ($\gtrsim 1$ mm for the conditions of Fig. 4). This naturally explains why in this case $L(0)$ is larger than when both SR and LR interactions are nonadditive. This interesting phenomenon certainly requires further careful investigation.

In conclusion, the competition between the SR and LR interactions is a generic process playing an important role in fluid phase separation occurring in different systems ranging from complex plasmas to colloidal dispersions. We believe that the onset of this process—where the discreteness effects play an essential role—requires separate particle-resolved studies focused on the comparison with the results of the coarse-grained approach.

We acknowledge financial support from DLR/BMWi (Grant No. 50WP0203), RFBR (Grant No. N08-02-00444-a), and DFG (SFB TR6).

*ivlev@mpe.mpg.de

[1] A. J. Bray, Adv. Phys. **51**, 481 (2002).
[2] D. G. A. L. Aarts *et al.*, New J. Phys. **7**, 40 (2005).
[3] A. E. Bailey *et al.*, Phys. Rev. Lett. **99**, 205701 (2007).
[4] A. K. Thakre, W. K. den Otter, and W. J. Briels, Phys. Rev. E **77**, 011503 (2008).
[5] M. Seul and D. Andelman, Science **267**, 476 (1995).
[6] A. Stradner *et al.*, Nature (London) **432**, 492 (2004).
[7] C. Sagui and R. C. Desai, Phys. Rev. E **49**, 2225 (1994).
[8] K. O. Ng and D. Vanderbilt, Phys. Rev. B **52**, 2177 (1995).
[9] C. P. Royall *et al.*, J. Phys. Condens. Matter **17**, S3401 (2005).
[10] V. E. Fortov *et al.*, Phys. Rep. **421**, 1 (2005).
[11] G. Morfill and A. Ivlev, Rev. Mod. Phys. **81**, 1353 (2009).
[12] S. A. Khrapak, B. A. Klumov, and G. E. Morfill, Phys. Rev. Lett. **100**, 225003 (2008).
[13] V. J. Anderson *et al.*, Nature (London) **416**, 811 (2002).
[14] E. D. Siggia, Phys. Rev. A **20**, 595 (1979).
[15] H. M. Thomas *et al.*, New J. Phys. **10**, 033036 (2008).
[16] See supplementary material at http://link.aps.org/supplemental/10.1103/PhysRevLett.105.045001 for Movies S1–S3 and simulation methodology.
[17] A. V. Ivlev *et al.*, Europhys. Lett. **85**, 45001 (2009).
[18] S. A. Khrapak *et al.*, Phys. Plasmas **17**, 042107 (2010).
[19] P. Hopkins *et al.*, J. Chem. Phys. **124**, 054503 (2006).
[20] H. Furukawa, Physica (Amsterdam) **123A**, 497 (1984).
[21] This value appears to be close to the prediction by K. Binder and D. Stauffer, Phys. Rev. Lett. **33**, 1006 (1974).
[22] I. M. Lifshitz *et al.*, J. Phys. Chem. Solids **19**, 35 (1961).
[23] D. A. Huse, Phys. Rev. B **34**, 7845 (1986).